Capacity of associative memory using a nonmonotonic neurons

Article *in* Neural Networks · December 1993

Impact Factor: 2.71 · DOI: 10.1016/0893-6080(93)90014-N · Source: DBLP

3 authors, including:

Shun-ichi Amari
RIKEN
522 PUBLICATIONS **22,741** CITATIONS

SEE PROFILE

Neural Networks, Vol. 6, pp. 167–176, 1993
Printed in the USA. All rights reserved.

0893-6080/93 $6.00 + .00

ORIGINAL CONTRIBUTION

Capacity of Associative Memory Using a Nonmonotonic Neuron Model

SHUJI YOSHIZAWA, MASAHIKO MORITA AND SHUN-ICHI AMARI

University of Tokyo

(*Received* 23 *January* 1992; *revised and accepted* 17 *July* 1992)

Abstract—*Associative memory using a sigmoid neuron model with the autocorrelation matrix has the advantage of the simplicity of its structure of the memory but has the disadvantage of the memory capacity. Its absolute capacity is asymptotically* $n/(2 \log n)$, *where n is the number of neurons. By computer simulation, Morita has recently shown that the performance of the associative memory is improved remarkably by replacing the usual sigmoid neuron with a nonmonotonic one, without sacrificing the simplicity. We use a piecewise linear model of the nonmonotonic neuron and investigate the existence and stability of equilibrium states of the recalling process. We derive two kinds of theoretical estimates of the absolute capacity. One estimate gives the upper bound of the absolute capacity* $0.5n$, *and the other gives the average value of the absolute capacity* $0.4n$. *These values fit well with computer simulations.*

Keywords—Autocorrelation-type associative memory, Capacity, Nonmonotonic neuron, Piecewise linear model, Equilibrium state, Stability.

1. INTRODUCTION

The neural network model of the autocorrelation associative memory or the content addressable memory has a long history of research (see, for example, Amari, 1972; Anderson, 1972; Kohonen, 1972; Nakano, 1972). Hopfield (1982) introduced the concept of the energy function being analogous with the spin-glass, and showed by computer simulation that the memory capacity of the associative memory is approximately $0.15n$, where n is the number of neurons. Namely, the autocorrelation associative memory can recall randomly generated patterns up to $0.15n$ with a small error. Since then a number of researchers studied the properties of the associative memory theoretically.

It has been proven that the absolute capacity is asymptotically $n/(2 \log n)$ (McEliece, Posner, Rodemich, & Venkatesh, 1987; Weisbuch, 1985), where the absolute capacity is the maximum number of randomly generated patterns which are memorized as the equilibria of the network with the correlation-type connection weights. On the other hand, Amit, Gutfreund, & Sompolinsky (1985a, 1985b) showed by using the replica method that the memory capacity is about $0.14n$ if a small percent of errors is admitted in the recalling process. This is called the relative capacity. Amari and Maginu (1988) studied the dynamical aspects of the recalling process by using the statistical neurodynamical method, where the relative capacity of $0.16n$ is obtained by a simple approximation method.

There are two flaws in the conventional associative memory model. The first one is that its absolute capacity of $n/(2 \log n)$ is smaller than n in order and its relative capacity of $0.15n$ is not large. The second one is the existence of a large number of spurious memories (Gardner, 1986).

There are a number of modifications of the prototype. They are, for example, the generalized-inverse memory matrix (Amari, 1977; Kohonen & Ruohonen, 1973), the optimal capacity by a general memory matrix (Gardner, 1988), the sparsely encoded associative memory (Amari, 1989; Meunier, Yanai, & Amari, 1991; Palm, 1980; Willshaw, Buneman, & Longuet-Higgins, 1969), introduction of sparsity in connections (Yanai, Sawada, & Yoshizawa, 1991), introduction of

Acknowledgments: The authors express their appreciation to Drs. N. Ito and N. Murata of the University of Tokyo for their valuable criticisms. The authors also thank Dr. K. Judd for checking the manuscript and offering advice. This study was partially supported by Grant-in-aid (#03234109, #03251102 and #03831003) of the Ministry of Education of Japan.

Requests for reprints should be sent to Shuji Yoshizawa, Department of Mathematical Engineering and Information Physics, Faculty of Engineering, University of Tokyo, 7-3-1 Hongo, Bunkyo, Tokyo 113, Japan.

excitatory and inhibitory neurons (Shinomoto, 1987), the chaos association memory (Aihara, Takabe, & Toyoda, 1990) and so on. However, these are not completely free from the above flaws.

Recently, Morita has shown that the performance of the conventional associative memory model is improved remarkably by replacing the usual sigmoid or hard-limiter neuron with a nonmonotonic neuron (Morita, Yoshizawa, & Nakano, 1990a, 1990b; see also Kobayashi, 1991, for a possible capacity of a single nonmonotonic neuron). A nonmonotonic neuron is an analog device whose output is a nonmonotonic function of its internal potential whose dynamics is governed by a first order differential equation. One remarkable fact is that the absolute capacity is about $0.4n$, which is much greater than the absolute capacity $n/(2 \log n)$ of the conventional model and is larger than even the relative capacity $0.15n$. The other point is the disappearance of the spurious memory. When the network fails to recall a correct memorized pattern, the state shows a chaotic behavior instead of falling into a spurious memory.

The purpose of this paper is a theoretical analysis of the potentiality of the autocorrelation associative memory. We study conditions which guarantee that randomly generated patterns to be memorized are equilibria of the network. We also show their dynamical stability. Through these studies we prove that the absolute capacity is about $0.4n$ and is upper bounded by $0.5n$, which is compatible with computer simulation. We adopt a piecewise linear model of the nonmonotonic neuron and also touch upon a theoretical explanation why spurious memories disappear.

2. AUTOCORRELATION ASSOCIATIVE MEMORY

In this section we give a short summary of the autocorrelation associative memory model and describe Morita's improvement on the recalling process.

This model consists of n neurons. Memorized patterns are n-dimensional random vectors whose elements take the values ± 1 randomly with equal probability and they are denoted by $\boldsymbol{s}^{(\mu)} = (s_1^{(\mu)} s_2^{(\mu)} \ldots s_n^{(\mu)})^T$ $(\mu = 1, 2, \ldots, m)$. The memory matrix W is constructed as follows,

$$w_{ij} = \frac{1}{n} \sum_{\mu=1}^{m} s_i^{(\mu)} s_j^{(\mu)} \quad (i \neq j)$$

$$w_{ii} = 0,$$

or in the matrix form,

$$W = \frac{1}{n} SS^T - aE_n, \tag{1}$$

where

$$S = [\boldsymbol{s}^{(1)} \boldsymbol{s}^{(2)} \ldots \boldsymbol{s}^{(m)}], \tag{2}$$

E_n is the n-dimensional unit matrix, S^T is the transpose of S, and a is the memory ratio defined by

$$a = \frac{m}{n}. \tag{3}$$

We can assume that the covariance matrix $S^T S$ is nonsingular. And also without loss of generality we can assume

$$\boldsymbol{s}^{(1)} = (1 \ldots 1)^T, \tag{4}$$

and analyze the recalling dynamics of $\boldsymbol{s}^{(1)}$.

The recalling dynamics is given by

$$\frac{d\boldsymbol{u}}{dt} = -\boldsymbol{u} + Wf(\boldsymbol{u}), \tag{5}$$

where $\boldsymbol{u} = (u_1 u_2 \ldots u_n)^T$ is an n-dimensional vector which represents the internal potential of neurons and f is the scalar output function of the neuron that operates on each element of the vector $\boldsymbol{u}$. Conventional associative memories use a sigmoid output function, however, the Morita model uses a nonmonotonic function as shown in Figure 1 (Morita et al., 1990a, 1990b).

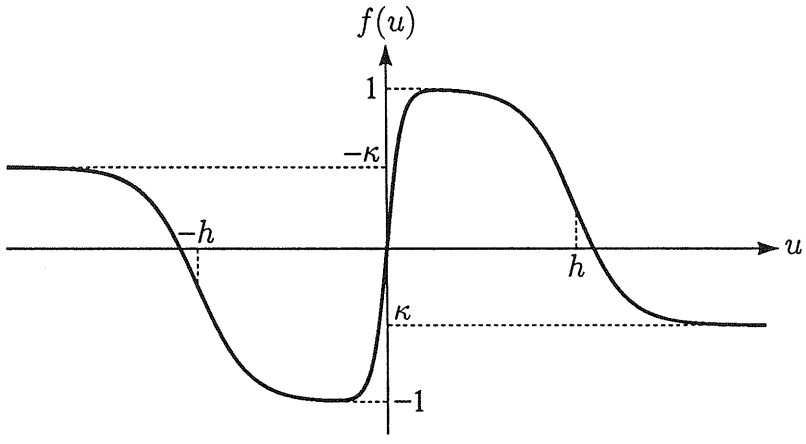

FIGURE 1. Non-monotonic output function.

The recalling process of the associative memory is as follows. For a given input pattern $\boldsymbol{u}_0$ we evaluate eqn (5) with initial condition $\boldsymbol{u}_0$ and if the solution converges to an equilibrium state $\boldsymbol{u}_e$, the recalled pattern is determined, not by $f(\boldsymbol{u}_e)$, but by the signum of $\boldsymbol{u}_e$: $\mathrm{sgn}(\boldsymbol{u}_e)$. If the solution does not converge, we cannot determine a recalled pattern and we deem that the recalling failed.

Comparisons of the recalling properties of the conventional and the nonmonotonic neurons are shown

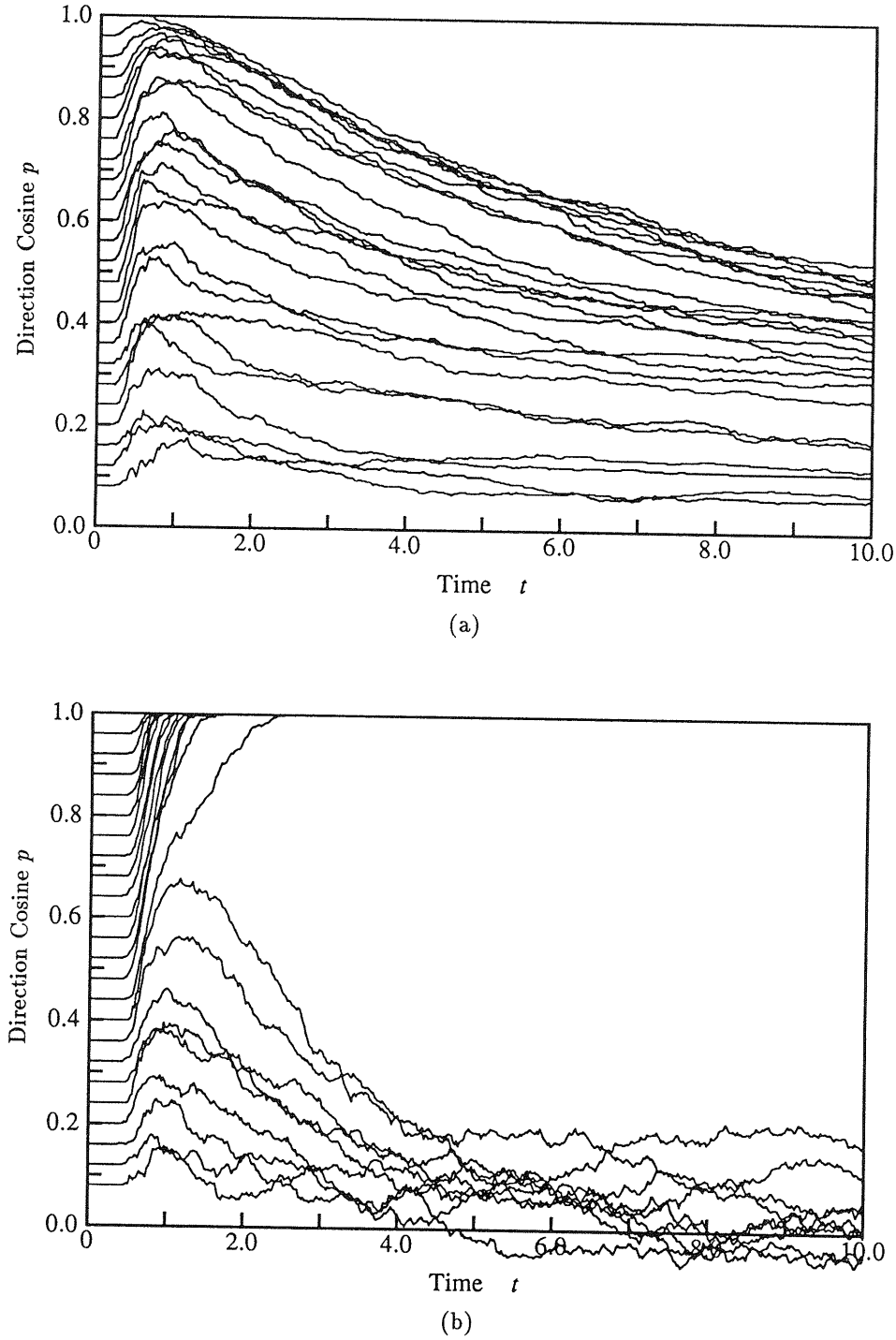

Figure 2. Time sequences of recalling process (n = 1000, a = 0.32). Abscissa and ordinate are the time and the direction cosine between the signum of u(t) and $\mathbf{s}^{(1)}$. Accordingly, the larger the direction cosine is, the closer to $\mathbf{s}^{(1)}$ the recalled pattern is. The direction cosines for the conventional neuron (a) converge to values far less than 1 even if their initial values are set close to 1. This fact means that the memorized pattern $\mathbf{s}^{(1)}$ is unstable. For a nonmonotonic neuron (b), there is a basin of attraction around $\mathbf{s}^{(1)}$, for this special example, the critical direction cosine is about 0.44.

in Figures 2 and 3. The values of the parameters of the output function (Figure 1) used in these simulations are $h = 0.5$, $\kappa = -1$, and the number of neurons $n = 1000$. Figure 2 shows time evolution of the recalling process with a memory ratio of 0.32, where abscissa and ordinate are the time and the direction cosine between the signum of $\boldsymbol{u}(t)$ and $\boldsymbol{s}^{(1)}$. Figure 2(a) shows that the direction cosines for the conventional neuron converge to values far less than 1 even if their initial values are set close to 1. This fact means that the memorized pattern $\boldsymbol{s}^{(1)}$ is unstable. For a nonmonotonic neuron (Figure 2(b)), it can be seen that there is a basin of attraction around $\boldsymbol{s}^{(1)}$, for this special example, the critical direction cosine is about 0.44. Figure 3 is a summary of the relation between the memory ratio and the critical direction cosine, from which it can be seen that the nonmonotonic model (curve B) is superior to the sigmoid model (curve A). For the benefit of comparison, a result for the sigmoid neuron with the generalized-inverse memory matrix is also shown by curve C. It should be noted that the recalling is perfect in the cases of the nonmonotonic model (B) and the generalized-inverse memory matrix (C), while recalled patterns include a small percent of errors in the conventional model (A).

A remarkable feature of Figure 2(b) is that the evolution of $\boldsymbol{u}$ does not converge to an equilibrium state when memorized pattern $\boldsymbol{s}^{(1)}$ cannot be recalled. This suggests that spurious memories are rare for the nonmonotonic neuron model.

3. EQUILIBRIUM STATE OF PIECEWISE LINEAR MODEL

For ease of theoretical investigation, we approximate the nonmonotonic function shown in Figure 1 by the piecewise linear function shown in Figure 4. By doing so we can obtain the absolute capacity or the maximum memory ratio within which there exists a stable equilibrium of eqn (5) in the same quadrant as the memorized pattern.

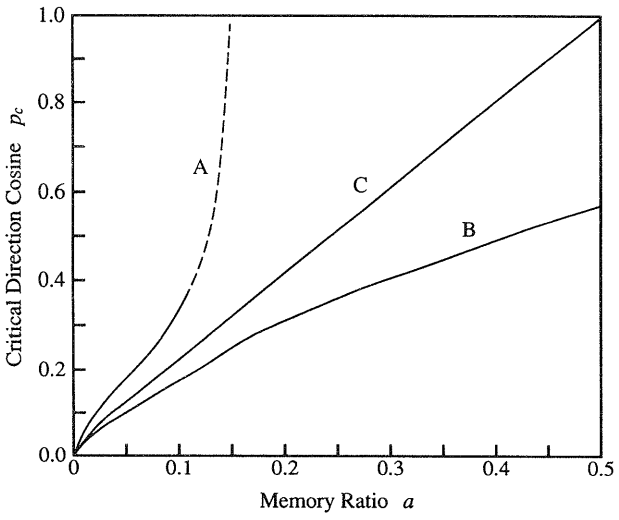

FIGURE 3. The relation between the memory ratio and the critical direction cosine. It can be seen that the nonmonotonic model (curve B) is superior to the sigmoid model (curve A). For the benefit of comparison, a result for the sigmoid neuron with the generalized-inverse matrix is also shown by curve C.

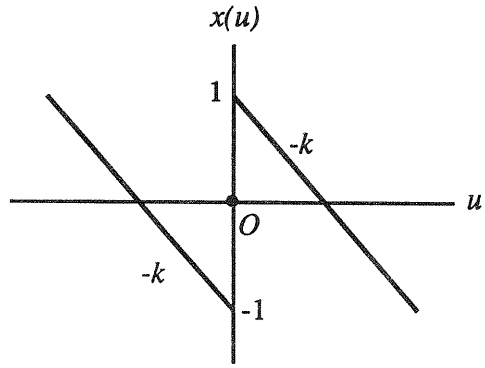

FIGURE 4. Piecewise linear approximation to nonmonotonic output function.

The recalling dynamics for the associative memory using the piecewise linear neuron is

$$\begin{cases} \dfrac{d\boldsymbol{u}}{dt} = -\boldsymbol{u} + W\boldsymbol{x}(\boldsymbol{u}), \\ \boldsymbol{x}(\boldsymbol{u}) = \operatorname{sgn}(\boldsymbol{u}) - k\boldsymbol{u}, \end{cases} \tag{6}$$

where sgn is the signum function defined by

$$\operatorname{sgn}(u) = \begin{cases} 1 & u \geq 0, \\ -1 & u < 0, \end{cases} \tag{7}$$

which operates on each element of the argument vector. Until Section 6 we assume that

$$k = \frac{1}{a}. \tag{8}$$

We have the following theorem.

THEOREM 1. *Let $\boldsymbol{u}$ be an equilibrium state of eqn (6) in the quadrant of the memorized pattern $\boldsymbol{s}^{(1)}$ and let $\boldsymbol{x} = -k\boldsymbol{u} + \operatorname{sgn}(\boldsymbol{u})$. Then the $\boldsymbol{x}$ is characterized by the following three conditions,*

$$\begin{aligned} &\text{(a)} \sum_{i=1}^{n} x_i s_i^{(\mu)} = 0 \quad (\mu = 2, 3, \ldots, \mathrm{m}), \\ &\text{(b)} \sum_{i=1}^{n} x_i s_i^{(1)} = \sum_{i=1}^{n} x = m. \\ &\text{(c)} \; x_i < 1 \quad (i = 1, 2, \ldots, n). \end{aligned} \tag{9}$$

Proof. The equilibrium state of eqn (6) is determined by

$$-\boldsymbol{u} + W\boldsymbol{x}(\boldsymbol{u}) = 0. \tag{10}$$

In the quadrant of $\boldsymbol{s}^{(1)}$ it holds that $\operatorname{sgn}(\boldsymbol{u}) = \boldsymbol{s}^{(1)}$. By substituting this relation, the second equation of eqn (6) and eqn (1) into eqn (10), we obtain

$$\frac{1}{k}\boldsymbol{s}^{(1)} - \left(\frac{1}{k} - a\right)\boldsymbol{x} = \frac{1}{n}SS^T\boldsymbol{x}.$$

By eqn (8), the above equation is reduced to the following.

$$\frac{1}{k}\boldsymbol{s}^{(1)} = \frac{1}{n}SS^T\boldsymbol{x}. \tag{11}$$

Equation (11) is rewritten as

$$S\left(\frac{1}{k} - \frac{1}{n}\alpha^{(1)} - \frac{1}{n}\alpha^{(2)} \ldots - \frac{1}{n}\alpha^{(m)}\right)^T = 0,$$

where

$$\alpha^{(\mu)} = \sum_{i=1}^{n} x_i s_i^{(\mu)} \quad (\mu = 1, 2, \ldots, m).$$

Taking into account that the covariance matrix S^TS is nonsingular, we have (a) and (b) of eqn (9). The condition (c) is equivalent with the condition that $\boldsymbol{x}$ is in the quadrant of $\boldsymbol{s}^{(1)}$. ■

The problem described in eqn (9) can be interpreted as follows. Firstly, vectors which satisfy condition (a) are contained in the orthocomplement of the subspace spanned by $\boldsymbol{s}^{(\mu)}$ ($\mu = 2, 3, \ldots, m$). Call this space Q. On the other hand, the vectors which satisfy conditions (b) and (c) form an n-polygon which is the intersection of the $(n-1)$-dimensional hyperplane defined by condition (b) and the semi-infinite region determined by $x_i \leq 1$ ($i = 1, 2, \ldots, n$). This region is illustrated in Figure 5 where it is the hatched area labeled B. Let R be an n-simplex whose vertices are those of B and the origin. The existence of an $\boldsymbol{x}$ which satisfies eqn (9) is equivalent to existence of an intersection of R and Q.

Since the $\boldsymbol{s}^{(\mu)}$ ($\mu = 1, 2, \ldots, m$) are assumed to be random vectors, we can determine the probability of existence of an $\boldsymbol{x}$ which satisfies eqn (9). The capacity of the associative memory is given by the minimum

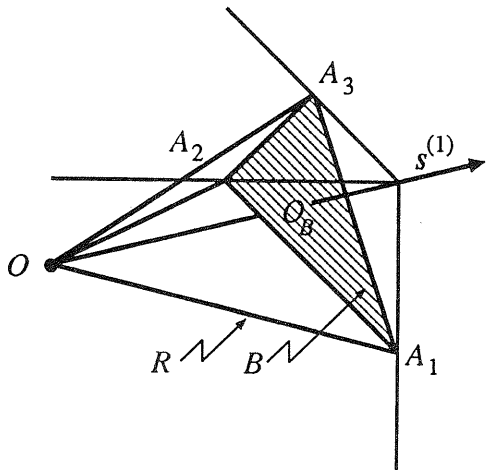

FIGURE 5. Geometrical representation of an equilibrium state. The hatched area illustrates the region of x which is determined by $\sum_{i=1}^{n} x_i s_i^{(1)} = m$, and $x_i < 1$.

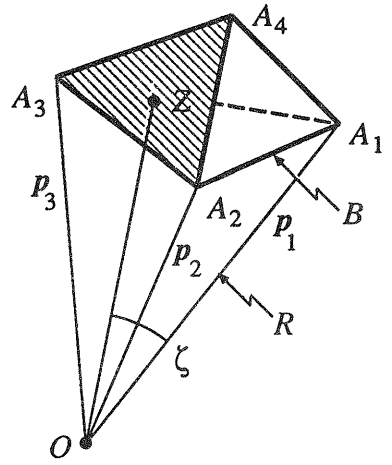

FIGURE 6. Caricature of the n-simplex R.

value of a for which the probability of existence of the $\boldsymbol{x}$ becomes 0 as number n of neurons increases to ∞.

If it is possible to approximate the simplex R by a cone with its vertex at the origin, then we can calculate the probability of the existence of the $\boldsymbol{x}$ from the following theorem. (Our calculation depends upon the assumption that $\boldsymbol{s}^{(\mu)}$ are distributed in every direction uniformly, though in the original formulation there are only a finite number of possible directions.)

THEOREM 2. *Let us fix an $(n - m + 1)$-dimensional subspace Q* in n-dimensional Euclidian space. If an n-*dimensional cone R with vertex at the origin and vertex angle $2\bar{\theta}$ is selected in a random direction, then the probability P of nonintersection of Q and R (other than at the origin) is given by*

$$P = \frac{\int_0^{\Theta} \sin^{n-m}\theta \cos^{m-2}\theta d\theta}{\int_0^{\pi/2} \sin^{n-m}\theta \cos^{m-2}\theta d\theta}, \tag{12}$$

where

$$\Theta = \frac{\pi}{2} - \bar{\theta}. \tag{13}$$

Proof. See Appendix A.

4. ESTIMATES OF THE VERTEX ANGLE OF THE n-SIMPLEX R

In this section, we introduce two estimates of the vertex angle of the n-simplex R.

4.1. Estimate by the Angle Between an Edge and its Facing Plane

The first estimate depends upon angle A_iOZ (denoted ζ_s), where A_i is any vertex of the n-polygon B, Z is any point on the facing plane of A_i and O is the origin (see Figure 6). In order to show more clearly the structure of the simplex, Figure 5 is redrawn as Figure 6 in which

base polygon B is represented as a tetrahedron. Coordinates of these points can be written as follows:

$$\begin{cases} A_1 : \boldsymbol{p}_1 = (m - n + 1, 1, 1, \ldots, 1)^T, \\ A_2 : \boldsymbol{p}_2 = (1, m - n + 1, 1, \ldots, 1)^T, \\ \qquad \cdots \\ A_n : \boldsymbol{p}_n = (1, \ldots, 1, 1, m - n + 1)^T, \end{cases} \tag{14}$$

$$\begin{cases} Z = (z_1, z_2, \ldots, z_n)^T, \\ z_1 = 1, \\ z_i = \sum_{j=2}^{n} \lambda_j p_{ij}, \quad (i = 2, \ldots, n), \\ \lambda_j \geq 0, \quad \sum_{j=2}^{n} \lambda_j = 1. \end{cases} \tag{15}$$

With these notations we have the following theorem.

THEOREM 3.

$$\lim_{n \to \infty} \zeta_s = \frac{\pi}{2}. \tag{16}$$

Proof. See Appendix B.

On the other hand, the coordinate of a point on the plane $A_1 A_2 \ldots A_{n-1}$ that contains A_1 can be written

$$\boldsymbol{m}_\lambda = \sum_{j=1}^{n-1} \lambda_j \boldsymbol{p}_j \quad \lambda_j \geq 0, \quad \sum_{j=1}^{n-1} \lambda_j = 1.$$

Therefore, we have

$$\cos \zeta \simeq \frac{\lambda_1}{\sqrt{\sum \lambda_j^2}},$$

and ζ takes any value between 0 and $\pi/2$.

From the above theorem we see that the angle of simplex R at the origin O is $\pi/2$ for any direction. So it is reasonable to adopt this value as $2\bar{\theta}$ in eqn (13).

It will be worth mentioning the following facts. For the circumscribed cone of R, it holds that

$$\cos \frac{\zeta}{2} = \frac{a}{(1 - a)\sqrt{n}} \left(1 + O\left(\frac{1}{n}\right)\right),$$

and so $\zeta \to \pi$ as $n \to \infty$. On the other hand, for the inscribed cone it holds that

$$\cos \frac{\zeta}{2} = 1 + O\left(\frac{1}{\sqrt{n}}\right),$$

and $\zeta \to 0$ as $n \to \infty$. Hence, both cones do not provide us with any information about the limiting value of a.

4.2. Estimate by a Cone Which has Same Solid Angle as Simplex R

In the above subsection we observed that when n is large, the vertex angle of the inscribed cone is zero but the angle between an edge and its facing plane is $\pi/2$. From this we can image a shape of the simplex such that edges of the simplex thrust out sharply. In order to get a more averaged criterion than the angle between an edge and its facing plane, we adopt a cone with a solid angle equal to that of the simplex.

Using Amari's method, we can calculate solid angle spanned by the simplex R (Amari, 1990).

THEOREM 4. *Let v_0 be the value of v at which the function*

$$\Psi(v, \sigma) = \frac{v^2}{2\sigma^2} - \log\{1 - \Phi(v)\} \tag{17}$$

takes its minimum, where $\Phi(v)$ is the error integral defined by

$$\Phi(v) = \int_{-\infty}^{v} \frac{1}{\sqrt{2\pi}} \exp\left\{-\frac{u^2}{2}\right\} du.$$

Then, when the number n of neurons is sufficiently large, the solid angle K_n spanned by the simplex R at the origin is given by the following equation,

$$K_n = C(v_0, \sigma) S_n \exp\left\{-n\left[\frac{v_0^2}{2\sigma^2} - \log\{1 - \Phi(v_0)\}\right]\right\}, \tag{18}$$

where

$$\sigma = \frac{\sqrt{1 - 2a}}{a}, \quad 0 \leq a \leq \frac{1}{2}, \tag{19}$$

S_n is the surface area of the n-dimensional unit sphere and $C(v, \sigma)$ is defined by

$$C(v, \sigma) = \frac{\sigma}{\sqrt{\sigma^2 + (\sigma^2 + 1)v^2}}.$$

Proof. See Appendix C.

COROLLARY 5. *If $2\theta_c$ is the vertex angle of a cone whose solid angle is equal to that given in Theorem 4, then*

$$\sin \theta_c = \exp\left\{-\left[\frac{v_0^2}{2\sigma^2} - \log\{1 - \Phi(v_0)\}\right]\right\}, \tag{20}$$

where v_0 is the same as in Theorem 4.

Proof. See Appendix D.

In order to see explicitly the relation between the memory ratio a and vertex angle θ_c, we have to solve eqn (20) numerically. However, the following two values are easily obtained,

$$a = 0 \to \theta_c = \frac{\pi}{2},$$

$$a = \frac{1}{2} \to \theta_c = \frac{\pi}{6}.$$

5. ESTIMATES OF THE MEMORY CAPACITY

In this section we calculate the capacity of the associative memory based upon the above obtained vertex an-

gles. Let us remark that the integrand of eqn (12),

$$\sin^{n-m}\theta \cos^{m-2}\theta,$$

is positive and takes its maximum value at

$$\bar{\theta}(a) = \arctan\sqrt{\frac{1-a}{a}}. \tag{21}$$

Also, the denominator of eqn (12) can be split into two terms as

$$\int_0^{\Theta} \sin^{n-m}\theta \cos^{m-2}\theta d\theta + \int_{\Theta}^{\pi/2} \sin^{n-m}\theta \cos^{m-2}\theta d\theta.$$

Using the saddle point approximation we can rewrite eqn (12) as follows,

$$P = \begin{cases} 0 & \Theta(a) < \tilde{\theta}, \\ 1 & \Theta(a) > \tilde{\theta}. \end{cases} \tag{22}$$

In the case of the vertex angle of the n-simplex, Theorem 3 gives the following Θ,

$$\Theta = \frac{\pi}{2} - \bar{\theta} = \frac{\pi}{2} - \frac{\pi}{4} = \frac{\pi}{4}.$$

Hence, we have

$$\tilde{\theta}(a) > \Theta \quad \text{for} \quad 0 \le a < \tfrac{1}{2}$$

and the memory capacity is estimated as 0.5.

On the other hand, in the case of the solid angle of the n-simplex, we have to solve eqn (20) numerically to get a function $\Theta = \Theta(a)$, which is compared with $\tilde{\theta}(a)$ as in Figure 7.

These results are summarized in the following corollary.

COROLLARY 6. *In the case of $k = a^{-1}$, an upper bound of the memory capacity is given by $0.5n$ and the average value is estimated at $0.398n$.*

In numerical calculations of eqn (6) for $n = 300$, we could get a correct recalling result for $a = 0.5$ by selecting proper initial values. But for $n = 1000$, the upper limit of a for correct recalling was between 0.4 and 0.41.

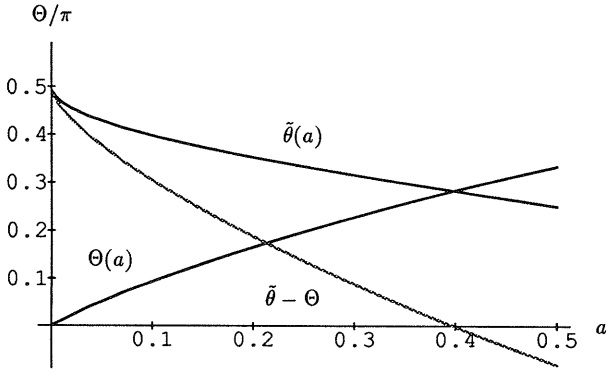

FIGURE 7. Capacity estimated by a cone with the same solid angle. The value of a at which $\tilde{\theta} - \Theta$ is equal to 0 gives the memory capcity.

6. THE CASE $k \neq a^{-1}$

In order to investigate the case where $k \neq a^{-1}$, we will consider the equilibrium solution for k nearly equal to a^{-1}. Using $\boldsymbol{x}$ we will rewrite eqn (6) as follows:

$$\frac{d\boldsymbol{x}}{dt} = -\frac{k_0 - k}{k_0}\boldsymbol{x} - \frac{k}{n}SS^T\boldsymbol{x} + \boldsymbol{s}^1, \tag{23}$$

where $k_0 = 1/a$ and $\boldsymbol{x}_0$ denotes the equilibrium solution given by eqn (11), that is, $\boldsymbol{x}_0$ satisfies

$$\frac{1}{k_0}\boldsymbol{s}^1 = \frac{1}{n}SS^T\boldsymbol{x}_0. \tag{24}$$

Then we have the following result concerning the solutions in the neighborhood of x_0.

THEOREM 7. *Assume that there exists the equilibrium solution $\boldsymbol{x} = \boldsymbol{x}_0$ defined in Theorem 1 with respect to the estimation by a cone. Then there exists an equilibrium solution for eqn (23) in the neighborhood of $\boldsymbol{x}_0$ if k is sufficiently close to k_0.*

Proof. See Appendix E.

By this theorem and Corollary 6, we can conclude that the memory capacity is close to $0.398n$ if k is close to k_0. For the analysis for k far from k_0, it seems necessary to know the statistical properties of $(S^TS)^{-1}$, which are very complicated.

7. STABILITY OF EQUILIBRIUM SOLUTIONS

In our piecewise linear model, stability of equilibrium solutions are easily determined if their locations are known. Namely, the variational equation at equilibrium solution $\boldsymbol{x} = \boldsymbol{x}_0$ is given by

$$\frac{d\boldsymbol{z}}{dt} = -\frac{k_0 - k}{k_0}\boldsymbol{z} - \frac{k}{n}SS^T\boldsymbol{z},$$

where $\boldsymbol{z} = \boldsymbol{x} - \boldsymbol{x}_0$.

In the coordinate system described in the Appendix E, this reduces to the following:

$$\frac{d\boldsymbol{\xi}}{dt} = -\frac{k_0 - k}{k_0}\boldsymbol{\xi} - \frac{k}{n}\begin{bmatrix} S^TS & 0 \\ 0 & 0 \end{bmatrix}\boldsymbol{\xi}. \tag{25}$$

Taking into consideration that S^TS is positive definite, we have the following results:

1. $\boldsymbol{x}_0$ is stable when $k < k_0$,
2. $\boldsymbol{x}_0$ is neutrally stable when $k = k_0$,
3. $\boldsymbol{x}_0$ is unstable when $k > k_0$. (This implies that directions of nonmemorized vectors are unstable.)

8. CONCLUDING REMARK

In this paper we investigated the recalling process of an autocorrelation associative memory whose neuron element has a nonmonotonic output function and derived its absolute capacity theoretically. It is worth

mentioning that the theoretical result shows good agreement with the numerical experiments. Also, we consider it a new result that the absolute capacity is of order n (nearly equal to $0.4n$), which contrasts with the relative capacity of order $0.15n$ obtained by numerical simulations for the sigmoid output neuron and that obtained by the replica theory for the signum output neuron, and the theoretical absolute capacity of order $n/(2 \log n)$ for the signum output neuron.

As for the spurious memory, it is possible to show the following properties theoretically. When $k = 1/a$, there is no spurious memory which contains a component orthogonal to the memorized patterns. As the value of k becomes smaller, the possibility of the existence of such kind of spurious memory increases.

Our consideration in this paper was restricted to the existence of equilibrium solutions and local stability. In order to get a complete understanding of the ability of the associative memory using the nonmonotonic neuron, we have to investigate further problems such as the size of the basin of attraction, the full sketch of spurious memories, and the behavior for clustered memorized patterns.

REFERENCES

Aihara, K., Takabe, T., & Toyoda, M. (1990). Bifurcation phenomena in nonlinear systems and theory of dynamical systems. *Physics Letters A,* **144,** 333–340.

Amari, S., & Maginu, K. (1988). Statistical neurodynamics of associative memory. *Neural Networks,* **1,** 63–73.

Amari, S. (1972). Learning patterns and pattern sequences by self-organizing nets of threshold elements. *IEEE Transactions on Computers,* **C-21**(11), 1197–1206.

Amari, S. (1977). Neural theory of association and concept-formation. *Biological Cybernetics,* **26,** 175–185.

Amari, S. (1989). Characteristics of sparsely encoded associative memory. *Neural Networks,* **2,** 451–457.

Amari, S. (1990). Mathematical foundations of neurocomputing. *Proceedings of the IEEE,* **78**(9), 1443–1463.

Amit, D. J., Gutfreund, H., & Sompolinsky, H. (1985a). Spin-glass models of neural networks. *Physical Review A,* **32,** 1007–1018.

Amit, D. J. Gutfreund, H., & Sompolinsky, H. (1985b). Storing infinite numbers of patterns in a spin-glass model of neural networks. *Physical Review Letters,* **55**(14), 1530–1533.

Anderson, J. A. (1972). A simple neural network generating an interactive memory. *Mathematical Biosciences,* **14,** 197–220.

Gardner, E. (1986). Structure of metastable states in the Hopfield model. *Journal of Physiology A,* **19,** 1047–1052.

Gardner, E. (1988). The space of interaction in neural network models. *Journal of Physics A: Math. Gen.,* **21,** 257–270.

Hopfield, J. J. (1982). Neural network and physical systems with emergent collective computational abilities. *Proceedings of the National Academy of Sciences, USA,* **79,** 2554–2558.

Kobayashi, K. (1991). On the capacity of a neuron with a non-monotone output function. *Network,* **2,** 237–243.

Kohonen, T. (1972). Correlation matrix memories. *IEEE Transactions on Computers,* **C-21**(4), 353–359.

Kohonen, T., & Ruohonen, M. (1973). Representation of associated data by matrix operators. *IEEE Transactions on Computers,* **C22**(7), 701–702.

McEliece, R. J., Posner, E. C., Rodemich, E. R., & Venkatesh, S. S. (1987). The capacity of the Hopfield associative memory. *IEEE Transaction Information Theory,* **IT-33**(4), 461–482.

Meunier, C., Yanai, H., & Amari, S. (1991). Sparsely coded associative memories: Capacity and dynamical properties. *Network,* **2**(4), 469–487.

Morita, M., Yoshizawa, S., & Nakano, K. (1990a). Analysis and improvement of the dynamics of autocorrelation associative memory. *Transactions on Institute Electronics, Information and Communication Engineers,* **J73-D-III**(2), 232–242.

Morita, M., Yoshizawa, S., & Nakano, K. (1990b). Memory of correlated patterns by associative neural networks with improved dynamics. *Proceedings INNC'90, Paris,* **2,** 868–871.

Nakano, K. (1972). Associatron—a model of associative memory. *IEEE Transactions on System, Man, Cybernetics,* **SMC-2,** 381–388.

Palm, G. (1980). On associative memory. *Biological Cybernetics,* **36,** 19–31.

Shinomoto, S. (1987). A cognitive and associative memory. *Biological Cybernetics,* **57,** 197–206.

Weisbuch, G. (1985). Scaling laws for the attractors of Hopfield networks. *Journal Physical Letters,* **46**(14), 623–630.

Willshaw, D. J., Buneman, O. P., & Longuet-Higgins, H. C. (1969). Non-holographic associative memory. *Nature,* **222,** 960–962.

Yanai, H., Sawada, Y., & Yoshizawa, S. (1991). Dynamics of an autoassociative neural network model with arbitrary connectivity and noise in the threshold. *Network,* **2**(3), 295–314.

APPENDIX

A. Proof of Theorem 2

At first, two notations are introduced.

$S_n(r)$: The surface area of n-dimensional sphere of radius $r(\sum_{i=1}^{n} \times x_i^2 \le r^2)$.

$S_{n,m}^{\bar{\theta}}$: The solid angle covered by the center line of a cone C whose vertex is at the origin and whose vertex angle is $2\bar{\theta}$, when the cone C moves in such a way that it has a nontrivial intersection with an $(n - m + 1)$-dimensional subspace Q.

LEMMA A.1. *The surface area of an n-dimensional sphere with radius r can be expressed as follows:*

$$S_n(r) = \int \frac{r}{\sqrt{r^2 - |\boldsymbol{x}|^2}} dx_2 \ldots dx_n, \tag{A.1}$$

where

$$|\boldsymbol{x}|^2 = \sum_{i=2}^{n} x_i^2 .$$

Proof. It is well known that $S_n(r)$ is expressed as follows:

$$S_n(r) = r^{n-1} \int_0^{\pi} \ldots \int_0^{\pi} \int_0^{2\pi} \sin^{n-2}\theta_1 \ldots \sin\theta_{n-2} d\theta_1 \ldots d\theta_{n-1}.$$

By changing the polar coordinates into the orthogonal coordinates

$$\begin{aligned} x_1 &= r\cos\theta_1, \\ x_2 &= r\sin\theta_1 \cos\theta_2, \\ &\cdots \\ x_{n-1} &= r\sin\theta_1 \ldots \sin\theta_{n-2}\cos\theta_{n-1}, \\ x_n &= r\sin\theta_1 \ldots \sin\theta_{n-2}\sin\theta_{n-1} \end{aligned}$$

the above integral can be rewritten as

$$S_n(r) = \int \frac{1}{\cos\theta_1} dx_2 \ldots dx_n,$$

since the Jacobian for the coordinate change is

$$J = (r^{n-1}\sin^{n-2}\theta_1 \ldots \sin\theta_{n-2}\cos\theta_1)^{-1}.$$

From this we have eqn. (A.1). ■

Now let us denote the $(m-1)$-dimensional subspace which is spanned by s^{μ} $(\mu = 2, \ldots, m)$ by $\boldsymbol{y} = (x_1, \ldots, x_{m-1})^T$ and its orthocomplement Q, which is an $(n-m+1)$-dimensional subspace, by $\boldsymbol{x} = (x_m, x_{m+1}, \ldots, x_n)^T$. Then noting that the solid angle $S^{\tilde{\theta}}_{n,m}$ is the surface area of that part of the unit sphere whose distance from Q is less than $\sin\tilde{\theta}$, we can write,

$$S^{\tilde{\theta}}_{n,m} = \int_{|\boldsymbol{x}|=\cos\tilde{\theta}}^{1} d\boldsymbol{x} \int_{(1-|\boldsymbol{x}|^2)\geq|\boldsymbol{y}|^2} \frac{d\boldsymbol{y}}{\sqrt{(1-|\boldsymbol{x}|^2)-|\boldsymbol{y}|^2}},$$

where $|\boldsymbol{x}|^2 = \sum_{i=m}^{n} x_i^2$, $|\boldsymbol{y}|^2 = \sum_{i=2}^{m-1} x_i^2$ and $d\boldsymbol{x} = dx_m \ldots dx_n$, $d\boldsymbol{y} = dx_2 \ldots dx_{m-1}$. By using eqn (A.1), we can rewrite the above as

$$\begin{aligned} S^{\tilde{\theta}}_{n,m} &= \int \frac{d\boldsymbol{x}}{\sqrt{1-|\boldsymbol{x}|^2}} \int \frac{\sqrt{1-|\boldsymbol{x}|^2}\,d\boldsymbol{y}}{\sqrt{(1-|\boldsymbol{x}|^2)-|\boldsymbol{y}|^2}} \\ &= \int \frac{d\boldsymbol{x}}{\sqrt{1-|\boldsymbol{x}|^2}} S_{m-1}(\sqrt{1-|\boldsymbol{x}|^2}) \\ &= \int (1-|\boldsymbol{x}|^2)^{m-3/2} d\boldsymbol{x} S_{m-1}(1). \end{aligned} \tag{A.2}$$

By changing $\boldsymbol{x}$ into polar coordinates $(\rho, \varphi_1, \ldots, \varphi_{n-m})$, we can rewrite the last integral of the above as

$$\int_{\rho=\cos\tilde{\theta}}^{1} (1-\rho^2)^{m-3/2} \rho^{n-m} d\rho \int_0^{\pi} \cdots \int_0^{\pi} \int_0^{2\pi} \times \sin^{n-m-1}\varphi_1 \ldots \sin\varphi_{n-m} d\boldsymbol{\varphi}.$$

Transformation $\rho = \cos\xi$ in this integral yields

$$\int_0^{\tilde{\theta}} \sin^{m-2}\xi \cos^{n-m}\xi d\xi S_{n-m+1}(1). \tag{A.3}$$

Then from eqns (A.2), (A.3), and (13), Theorem 2 follows.

B. Proof of Theorem 3

In the notations (14) and (15), the angle A_1OZ (denoted ζ_s) satisfies the following relation:

$$\cos\zeta_s = \frac{1}{\sqrt{1+\sum_{i=2}^{n} z_i^2}} \frac{(m-n+1)z_1 + \sum_{i=2}^{n} z_i}{\sqrt{(m-n+1)^2+n-1}}. \tag{B.1}$$

Note that coordinates z_i satisfy

$$\sum_{i=2}^{n} z_i = \sum_{j=2}^{n} \lambda_j \sum_{i=2}^{n} p_j^i = m-1, \tag{B.2}$$

and

$$\sum_{i=2}^{n} z_i^2 \geq \frac{(\sum_{i=2}^{n} z_i)^2}{n-1} = \frac{(m-1)^2}{n-1}. \tag{B.3}$$

Then from relations (B.1), (B.2), and (B.3), we have

$$|\cos\zeta_s| \leq \frac{1}{\sqrt{1+\dfrac{(m-1)^2}{n-1}}} \frac{m-1}{\sqrt{(m-n+1)^2+n-1}}.$$

If we put $m = an$, then

$$|\cos\zeta_s| \simeq \left|\frac{2a-1}{(1-a)a\sqrt{n}}\right| \to 0 \quad \text{as} \quad n \to \infty.$$

Hence, we get $\zeta_s \to \pi/2$.

C. Proof of Theorem 4

Let us use notation (14) again and define a region R^{∞} which is the positive convex hull of $\boldsymbol{p}_i$ $(i = 1, \ldots, n)$ defined by,

$$R^{\infty} = \left\{\boldsymbol{x} \middle| \boldsymbol{x} = \mu \sum_{i=1}^{n} \lambda_i \boldsymbol{p}_i, \sum_{i=1}^{n} \lambda_i = 1, \lambda_i \geq 0, \mu \geq 0\right\}.$$

Moreover, let us introduce an n-dimensional random vector $\boldsymbol{u} = (u_1, \ldots, u_n)^T$ whose components u_i are mutually independent and obey a normal distribution $N(0, 1)$. We will denote $P_{R^{\infty}}$ the probability that the random vector $\boldsymbol{u}$ is contained in the region R^{∞}.

The solid angle K_n spanned by the simplex R is equal to the probability $P_{R^{\infty}}$ multiplied by the surface area of the n-dimensional unit sphere. Vectors $\boldsymbol{e}_i$, which are normalization of $\boldsymbol{p}_i$ in (14), have the following direction cosines

$$\begin{aligned} \cos(\boldsymbol{e}_i, \boldsymbol{e}_j) &= \frac{2m-n}{(m-n+1)^2+n-1} \\ &= \frac{1}{n}\frac{2a-1}{(1-a)^2}\left(1+O\left(\frac{1}{n}\right)\right). \end{aligned} \tag{C.1}$$

Hence, we can orthogonalize them by introducing the following transformation

$$\tilde{\boldsymbol{e}}_i = \boldsymbol{e}_i - \frac{c}{n}\sum_{i=1}^{n} \boldsymbol{e}_i, \tag{C.2}$$

$$c = \begin{cases} \dfrac{2a-1}{a} & (<0) \quad \left(0 < a < \dfrac{1}{2}\right), \\ \dfrac{1}{a} & (>0) \quad \left(a > \dfrac{1}{2}\right), \end{cases} \tag{C.3}$$

so that

$$\tilde{\boldsymbol{e}}_i \cdot \tilde{\boldsymbol{e}}_i = \delta_{ij}.$$

Under the transformation (C.2), the random variables u_i are transformed to

$$\tilde{u}_i = u_i - \frac{c}{n}\sum_{i=1}^{n} u_i. \tag{C.4}$$

These new random variables $\tilde{u}_i$ are not mutually independent and have correlations,

$$\begin{aligned} E(\tilde{u}_i\tilde{u}_j) &= \frac{(c-2)c}{n} \\ &= \frac{1-2a}{na^2}. \end{aligned} \tag{C.5}$$

Thus, $\tilde{u}_i$ can be written as

$$\tilde{u}_i = u_i + \frac{1}{\sqrt{n}} v, \tag{C.6}$$

where v is a normal random variable with mean 0 and variance $\sigma = \sqrt{1-2a}/a$ (where the case $a > \frac{1}{2}$ is not treated here) and so

$$v \in N(0, \sigma^2),$$

$$\sigma^2 = \frac{1-2a}{a^2}.$$

After the transformation (C.2), the probability that $\boldsymbol{u} = (u_1 \ldots u_n)^T$ is contained in R^{∞} becomes the probability that $\tilde{\boldsymbol{u}} = (\tilde{u}_1 \ldots \tilde{u}_n)^T$ is contained in the positive convex hull of $\tilde{\boldsymbol{e}}_i$ $(i = 1, \ldots, n)$, namely $\tilde{u}_i > 0$ for all i. Therefore, we have

$$\begin{aligned} \frac{K_n}{S_n} &= P_{R^{\infty}} = \Pr(\tilde{u}_i > 0; \forall i) \\ &= E_v\left(\prod_{i=1}^{n}\left(1-\Phi\left(\frac{v}{\sqrt{n}}\right)\right)\right) \\ &= \frac{\sqrt{n}}{\sqrt{2\pi}\sigma}\int_{-\infty}^{\infty} \exp\left\{-n\left[\frac{v^2}{2\sigma^2} - \log\{1-\Phi(v)\}\right]\right\} dv \end{aligned} \tag{C.7}$$

By the application of the saddle point approximation method to the last integral of eqn (C.7), we have

$$\frac{K_n}{S_n} = \frac{\sqrt{n}}{\sqrt{2\pi}\sigma}$$

$$\times \exp\left\{-n\left[\frac{v_0^2}{2\sigma^2} - \log\{1 - \Phi(v_0)\}\right]\right\} \sqrt{\frac{2\pi}{n\Psi''(v_0, \sigma)}} \quad \text{(C.8)}$$

where v_0 and Ψ are defined in Theorem 4, and $''$ denotes the second derivative. Thus, we get eqn (18).

D. Proof of Corollary 5

The solid angle of a cone with vertex angle equal to $2\theta_c$ satisfies the following equation:

$$\int_0^{\theta_c}\int_0^{\pi}\cdots\int_0^{\pi}\int_0^{2\pi} \sin^{n-2}\theta_1 \ldots \sin\theta_{n-1} d\theta_1 \ldots d\theta_{n-1} \quad \text{(D.1)}$$

$$= S_{n-1}\int_0^{\theta_c} \sin^{n-2}\theta_1 d\theta_1. \quad \text{(D.2)}$$

Therefore, the vertex angle $2\theta_c$ of a cone whose solid angle is equal to that given in Theorem 4 is obtained from the relation,

$$\exp\left\{-n\left[\frac{v_0^2}{2\sigma^2} - \log\{1 - \Phi(v_0)\}\right]\right\}$$

$$= \frac{S_{n-1}}{S_n}\frac{1}{C(v_0, \sigma)}\int_0^{\theta_c} \sin^{n-2}\theta_1 d\theta_1, \quad \text{(D.3)}$$

where v_0 and $C(v, \sigma)$ are defined in Theorem 4.

Now let us note that we can construct a sequence of C^∞ functions $s_k(\theta)$ such that

$$s_k(\theta) = \begin{cases} \sin\theta & \left|\theta - \dfrac{\theta_c}{2}\right| \le \dfrac{\theta_c}{2} - \dfrac{1}{k}, \\ 0 & \left|\theta - \dfrac{\theta_c}{2}\right| \ge \dfrac{\theta_c}{2}, \end{cases} \quad \text{(D.4)}$$

$$0 < s_k(\theta) < \sin\theta \quad \theta < \theta < \frac{1}{k} \quad \text{or} \quad \theta_c - \frac{1}{k} < \theta < \theta_c,$$

and $s_k^n(\theta)$ are polynomial order in k, and

$$s_k(\theta) \to s(\theta) \equiv \begin{cases} \sin\theta & 0 \le \theta \le \theta_c, \\ 0 & \theta_c < \theta \le \pi/2, \end{cases} \quad \text{(D.5)}$$

as $k \to \infty$. For example, we can use

$$s_k(\theta) = \frac{\rho(\theta_c\theta - \theta^2)\sin\theta}{\rho(\theta_c\theta - \theta^2) + \rho\left(\theta^2 + \theta_c\theta + \dfrac{\theta_c}{k} - \dfrac{1}{k^2}\right)}, \quad \text{(D.6)}$$

where ρ is defined by

$$\rho(t) = \begin{cases} \exp(-1/t) & t > 0, \\ 0 & t \le 0. \end{cases}$$

Then, the integral of the right hand side of eqn (D.3) is approximated by

$$\int_0^{\pi/2} s_k^{n-2}(\theta)d\theta = \int_0^{\pi/2} \exp\{(n-2)\log s_k(\theta)\}d\theta. \quad \text{(D.7)}$$

Since $s_k(\theta)$ has its maximum at a θ (which is denoted θ_0) in the interval $(\theta_c - 1/k, \theta_c)$, we can apply the saddle point approximation method and the value of the integral (D.7) is given by

$$s_k^{n-2}(\theta_0)\sqrt{\frac{2\pi}{-(n-2)s_k''(\theta_0)}}. \quad \text{(D.8)}$$

Lastly, if we note that the maximum point θ_0 approaches θ_c and hence $s_k(\theta_0)$ approaches $\sin\theta_c$ and that the factor S_{n-1}/S_n satisfies

$$\log\frac{S_{n-1}}{S_n} = o(n),$$

we have eqn (20) by taking log of eqn (D.3).

E. Proof of Theorem 7

Substituting for $\boldsymbol{x}_0$ in eqn (23) by eqn (24) we have

$$\frac{d\boldsymbol{x}}{dt} = -\frac{k_0 - k}{k_0}\boldsymbol{x} - \frac{k}{n}SS^T\boldsymbol{x} + \frac{k_0}{n}SS^T\boldsymbol{x}_0. \quad \text{(E.1)}$$

Introduce the following coordinate transformation,

$$T = [SU]^{-1}, \quad \xi = T\boldsymbol{x}, \quad \xi_0 = T\boldsymbol{x}_0, \quad \text{(E.2)}$$

where S is the matrix defined in eqn (2) and U is a matrix which is composed of the basis vectors $\{\boldsymbol{u}^\nu, \nu = 1, \ldots, n-m\}$ of the orthocomplement of the subspace spanned by $\{\boldsymbol{s}^\mu, \mu = 1, \ldots, m\}$. By these coordinates, eqn (E.1) can be expressed,

$$\frac{d\xi}{dt} = -\frac{k_0 - k}{k_0}\xi - \frac{k}{n}\begin{bmatrix} G & 0 \\ 0 & 0 \end{bmatrix}\xi + \frac{k_0}{n}\begin{bmatrix} G & 0 \\ 0 & 0 \end{bmatrix}\xi_0, \quad \text{(E.3)}$$

where

$$G = S^TS.$$

Let $\hat{\xi}$ denote a vector formed from the first m components of ξ, and $\check{\xi}$ be formed from the remaining $n - m$ components. Then eqn (E.3) can be expressed in a form with two isolated parts:

$$\begin{cases} \dfrac{d\hat{\xi}}{dt} = -\dfrac{k_0 - k}{k_0}\hat{\xi} - \dfrac{k}{n}G\hat{\xi} + \dfrac{k_0}{n}G\hat{\xi}_0, \\ \dfrac{d\check{\xi}}{dt} = -\dfrac{k_0 - k}{k_0}\check{\xi}. \end{cases} \quad \text{(E.4)}$$

Therefore, the equilibrium solution satisfies

$$\begin{cases} \left(\dfrac{k_0 - k}{k_0}E_m + \dfrac{k}{n}G\right)\bar{\xi} = \dfrac{k_0}{n}G\hat{\xi}_0, \\ \check{\xi} = 0. \end{cases} \quad \text{(E.5)}$$

Thus,

$$\begin{cases} \hat{\xi} = \hat{\xi}_0 + O(k - k_0), \\ \check{\xi} = 0, \end{cases} \quad \text{(E.6)}$$

when $k \to k_0$. Hence, the equilibrium solution of eqn (E.1) tends to

$$\bar{\xi}_0 = \begin{bmatrix} \hat{\xi}_0 \\ 0 \end{bmatrix}, \quad \text{(E.7)}$$

as $k \to k_0$.

Now observe that $\mathbf{R}^n$ can be decomposed into the direct sum,

$$\mathbf{R}^n = \Xi' \oplus V \oplus U, \quad \text{(E.8)}$$

where Ξ' is an $(m-1)$-dimensional subspace spanned by $\boldsymbol{s}^2, \ldots, \boldsymbol{s}^m$, U is the $(n-m)$-dimensional orthocomplement of the subspace Ξ spanned by $\boldsymbol{s}^1, \ldots, \boldsymbol{s}^m$, and V is the one-dimensional ortho-complement of Ξ' in Ξ. In this decomposition $\bar{\xi}_0$ is expressed as

$$\alpha\boldsymbol{v},$$

where $\boldsymbol{v}$ is the basis of V. The orthogonal projection onto $Q = V \cup U$ maps the center line $\boldsymbol{s}^1$ of the cone onto $\bar{\xi}_0$, since $\boldsymbol{s}^1$ is orthogonal to U.

On the other hand, the equilibrium solution $\boldsymbol{x}_0$ given in Theorem 1 has the form

$$\alpha\boldsymbol{v} + \boldsymbol{u} \ (\boldsymbol{u} \in U).$$

Since a cone is convex and symmetric with respect to its center line, the point $\alpha\boldsymbol{v} - \boldsymbol{u}$ is also included in the intersection of the cone and Q, and hence the middle point $\alpha\boldsymbol{v}$ is included in the intersection. Hence, $\bar{\xi}_0$ is in the intersection.